

## Constructing Chiral Gold Nanorod Oligomers Using Spatially Separated Sergeants-and-Soldiers Effect

*Dejing Meng<sup>a,b</sup>, Xu Li<sup>c</sup>, Xinshuang Gao<sup>a,b</sup>, Chenqi Zhang<sup>a,b</sup>, Yinglu Ji<sup>a</sup>, Zhijian Hu<sup>a</sup>,*

*Lingling Ren<sup>c</sup> and Xiaochun Wu<sup>\*a,b</sup>*

### Supporting Information

#### Materials

Chloroauric acid ( $\text{HAuCl}_4 \cdot 3\text{H}_2\text{O}$ ), silver nitrate ( $\text{AgNO}_3$ ) were purchased from Beijing Chemical Reagent Company. Trisodium citrate was purchased from Alfa Aesar. L/D-cysteine (L/D-Cys), 4-aminophenol (4-ATP), mercaptobenzene (MB), sodium borohydride ( $\text{NaBH}_4$ ), cetyltrimethylammonium bromide (CTAB), L-ascorbic acid (AA) were purchased from Sigma. Milli-Q Water ( $18 \text{ M}\Omega \cdot \text{cm}$ ) was used for the experiments. Cetylpyridinium chloride (CPC) was purchased from Ark pharm. Cetyltrimethylammonium chloride (CTAC) was purchased from TCI.

#### Characterizations.

CD measurements were conducted on a JASCO J-1500 CD spectrometer and the bandwidth was set at 2 nm. Zeta potentials were obtained using a zeta potential and size analyzer (Malvern, Zeta-sizer nano ZS). Extinction spectra were obtained using a Cary 60 UV-vis-NIR spectrophotometer. SEM images were taken using a Zeiss JC-Merlin SEM with a voltage of 5 kV. TEM measurement was performed on a Tecnai G2 20 S-TWIN TEM at an accelerating voltage of 200 kV. Raman spectra were obtained in solution phase using a Renishaw InVia Raman microscope with a 785 nm laser. HRTEM images with relative strain mapping were taken using Titan G2 60-300 with image corrector (point resolution = 80 pm) operating at an accelerating voltage of 300 kV. Image analysis was done using GPA and Digital Micrograph (Gatan) software.

Spectra measurement: All extinction and CD spectra were obtained directly with solution samples in a 1 cm \* 1 cm quartz cuvette.

#### Experimental results

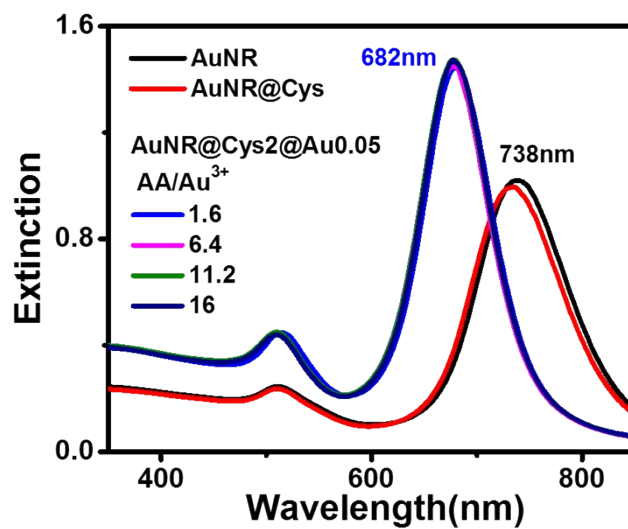


**Figure S1.** Effect of AA/Au<sup>3+</sup> molar ratio on extinction spectra of AuNR@Cys2@Au0.05 monomers.

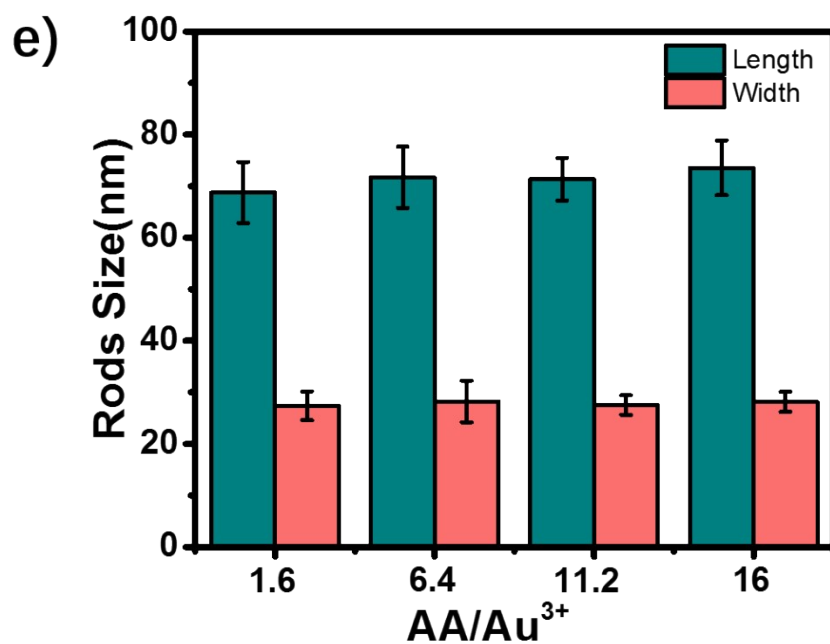
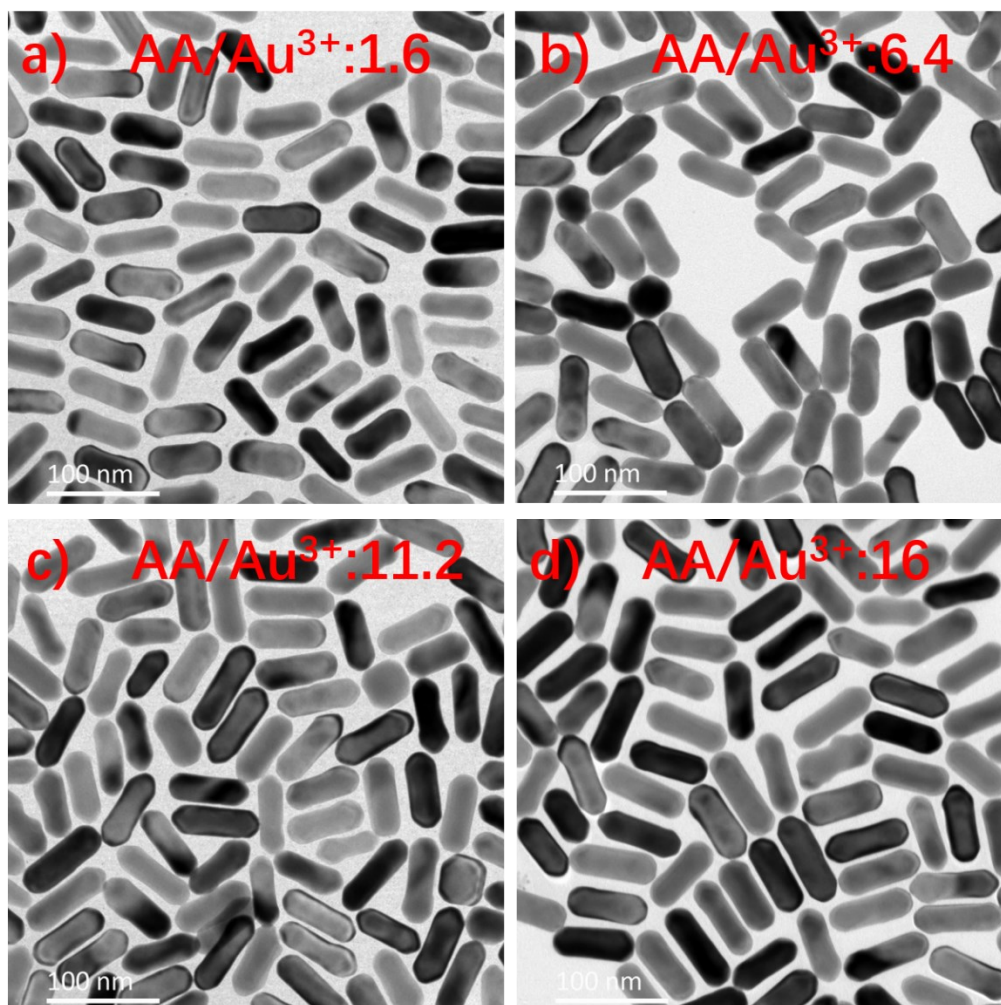


**Figure S2.** TEM images (a-d) of Au@Cys2@Au0.05 monomers obtained with different AA/Au<sup>3+</sup> ratios. (e) rod size vs AA/Au<sup>3+</sup> ratio.

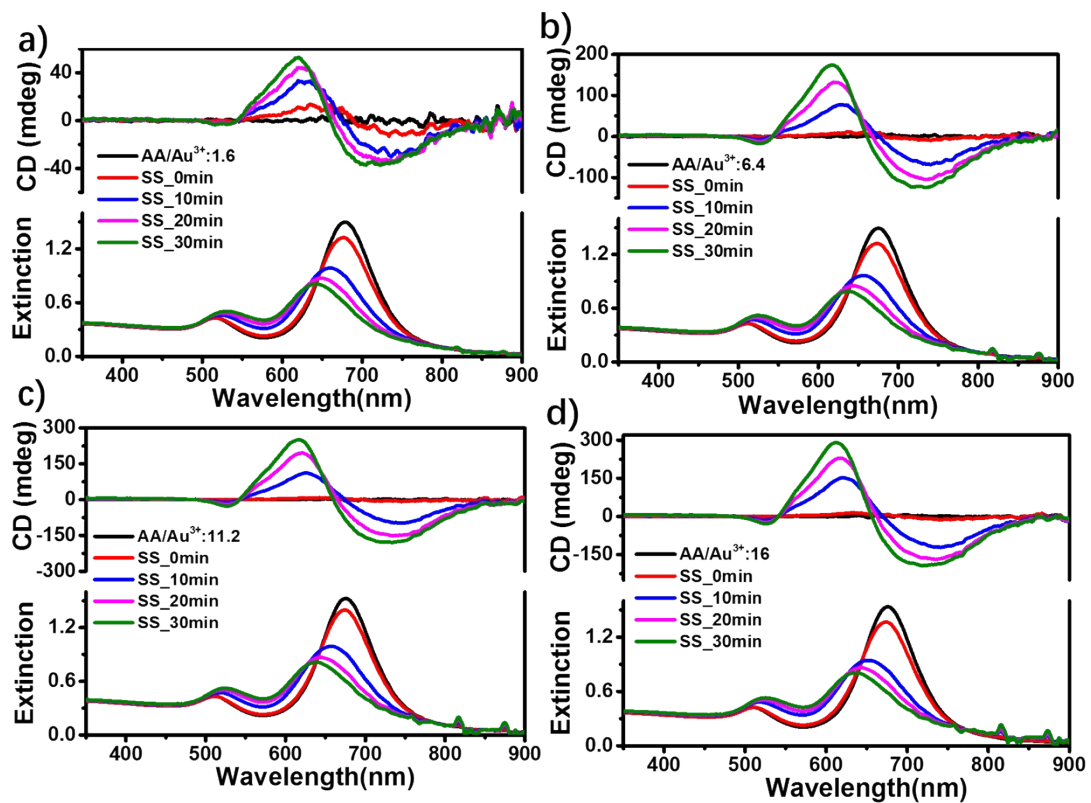


**Figure S3.** Changes in CD and extinction spectra of AuNR@Cys2@Au0.05 SS oligomers during 60 °C assembly process using monomers prepared with different AA/Au<sup>3+</sup> ratios.



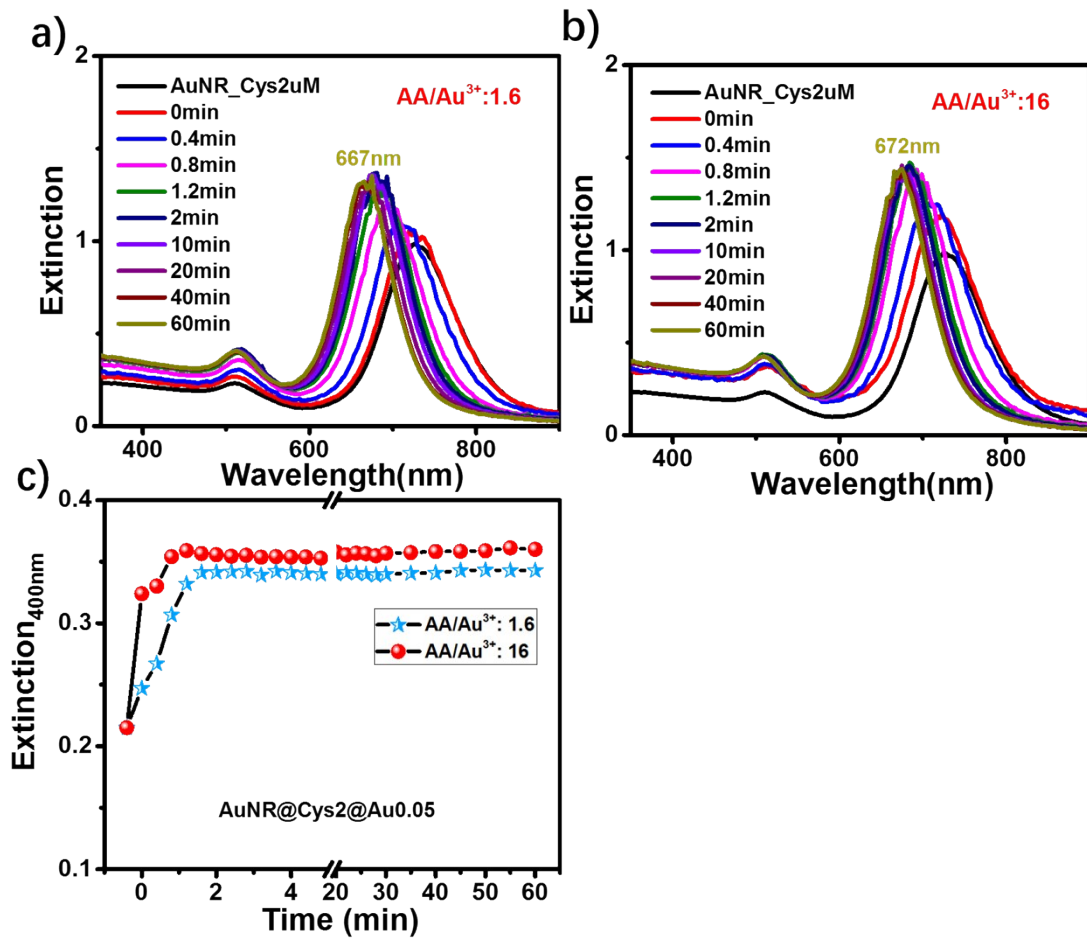


**Figure S4.** The evolutions (a, b) of extinction spectra of Au@Cys2@Au0.05 monomers during the overgrowth with AA/Au<sup>3+</sup> ratios of 1.6 and 16, respectively. (c) Extinction value at 400 nm vs Au shell growth time.

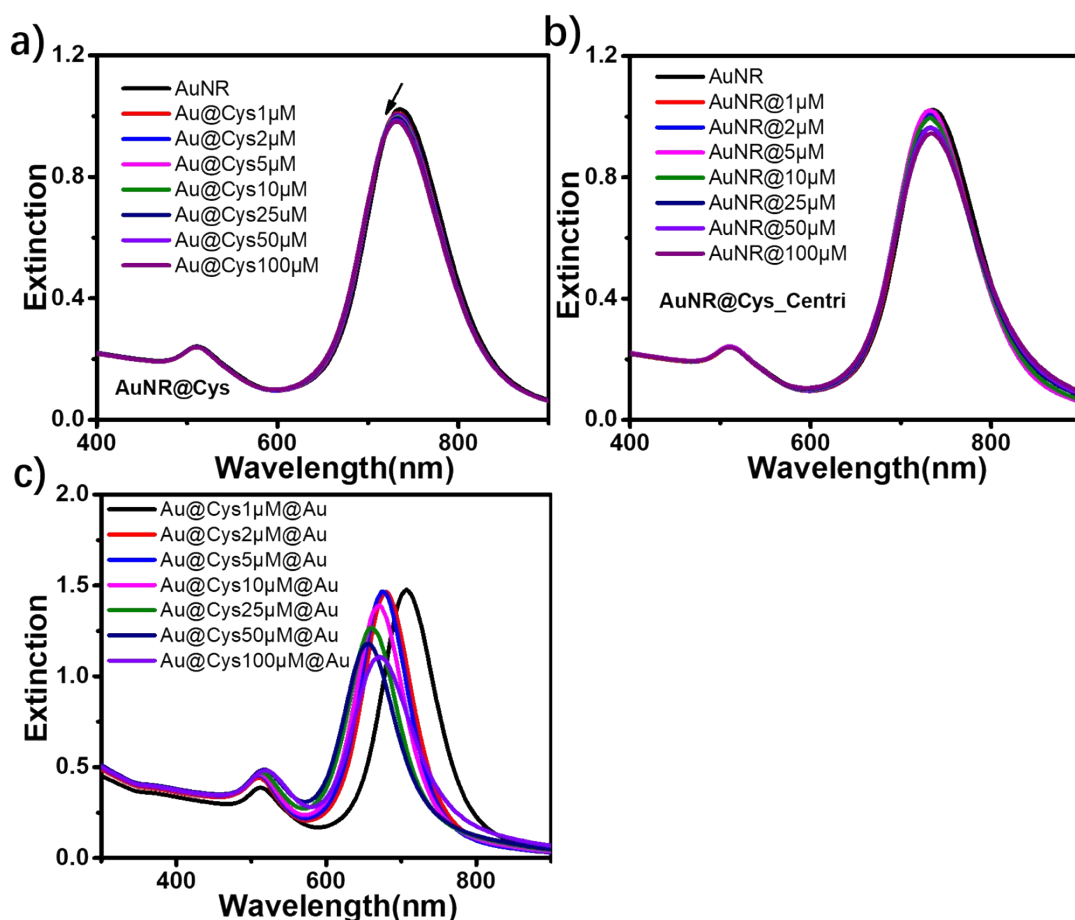


**Figure S5.** Extinction spectra of AuNRs incubated with different concentrations of cysteine before (a) and after (b) centrifugation and those of AuNR@CysX@Au0.05 after Au overgrowth (c).

Increasing Cys incubation concentration from 1  $\mu\text{M}$  to 100  $\mu\text{M}$ , the longitudinal SPR band showed a slight blue-shift and intensity damping, indicating that more Cys molecules adsorbed on the Au core surface (Fig.S5a). After centrifugation, AuNR@Cys monomers with  $[\text{Cys}] \geq 10 \mu\text{M}$  exhibited a slight aggregation, as witnessed by a long wavelength tailing and LSPR intensity decreasing (Fig.S5b). After Au shell overgrowth, the effect of Cys concentration was more obvious. The longitudinal SPR band showed a blue-shift trend with decreased intensity upon increasing Cys incubation concentration (Fig.S5c).

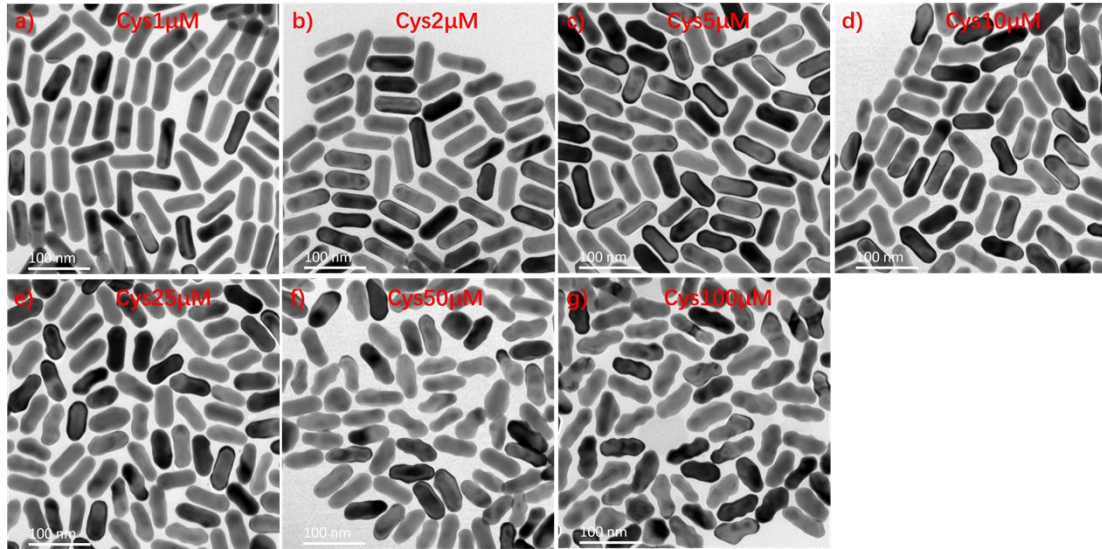


**Figure S6.** TEM images of AuNR@CysX@Au0.05 monomers.

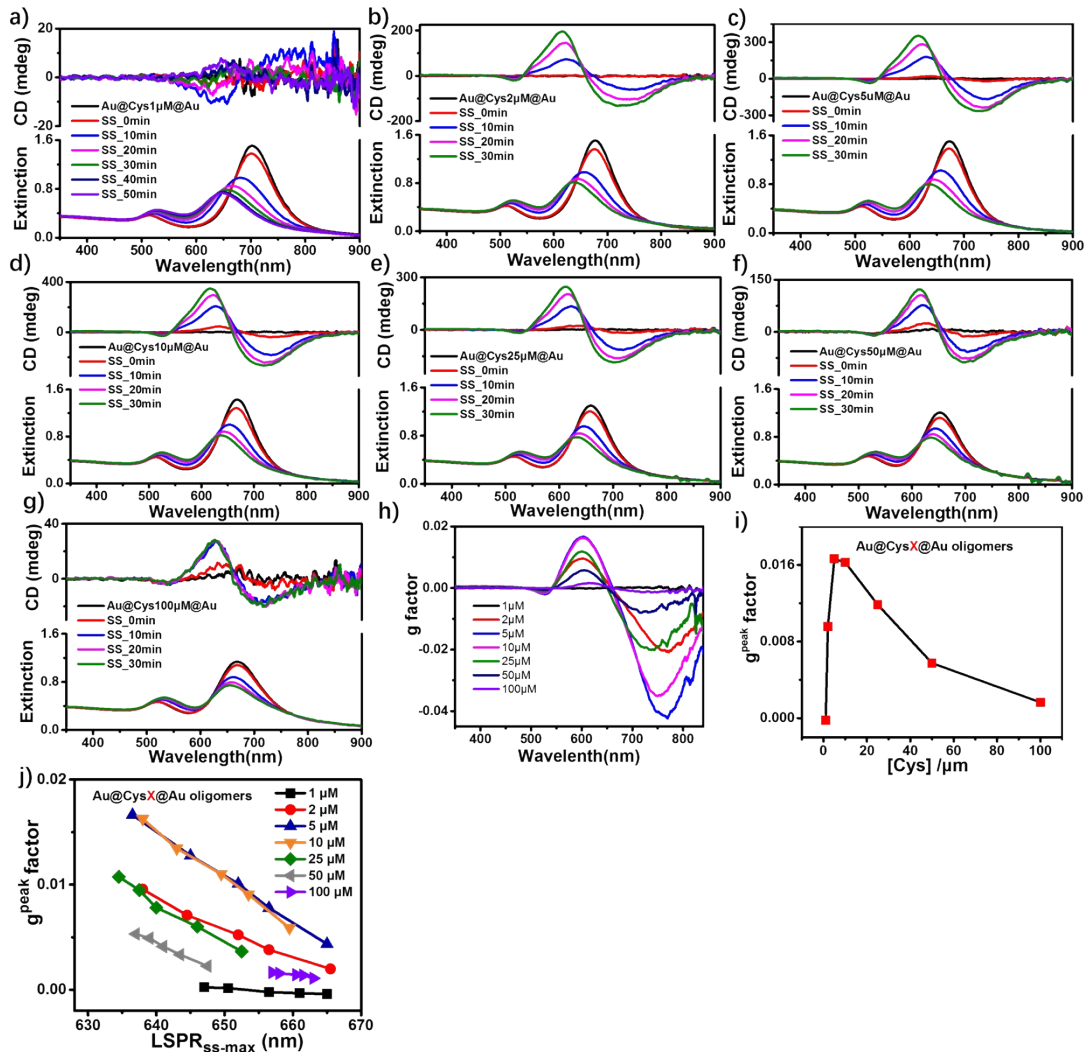


**Figure S7.** Effect of Cys incubation concentration on the PCD responses of AuNR@CysX@Au0.05 oligomers. (a-g) Evolution of CD and extinction spectra of Au@CysX@Au0.05 oligomers during

SS assembly processes at 60°C. (h) g factor spectra. (i) The  $g^{\text{peak}}$  value after 30 min assembly vs Cys concentration. (j) Relationship between  $g^{\text{peak}}$  value and  $\text{LSPR}_{\text{SS-max}}$ .

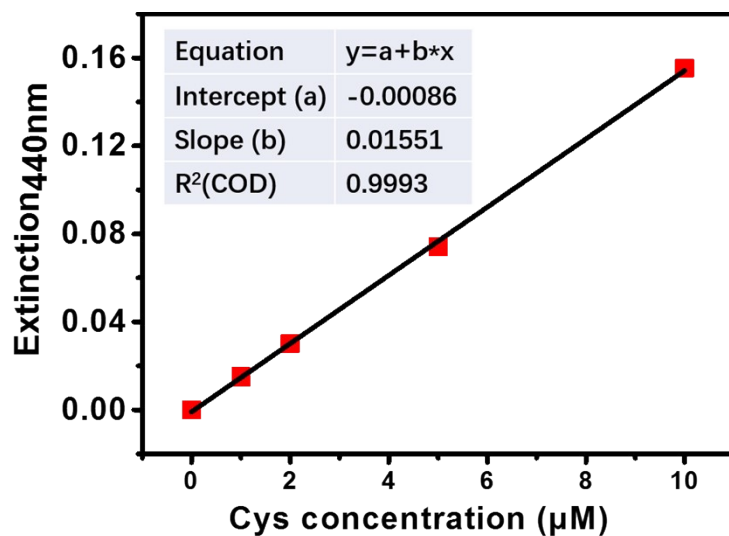


Figure S8. Standard curve for determining Cys adsorption amount.

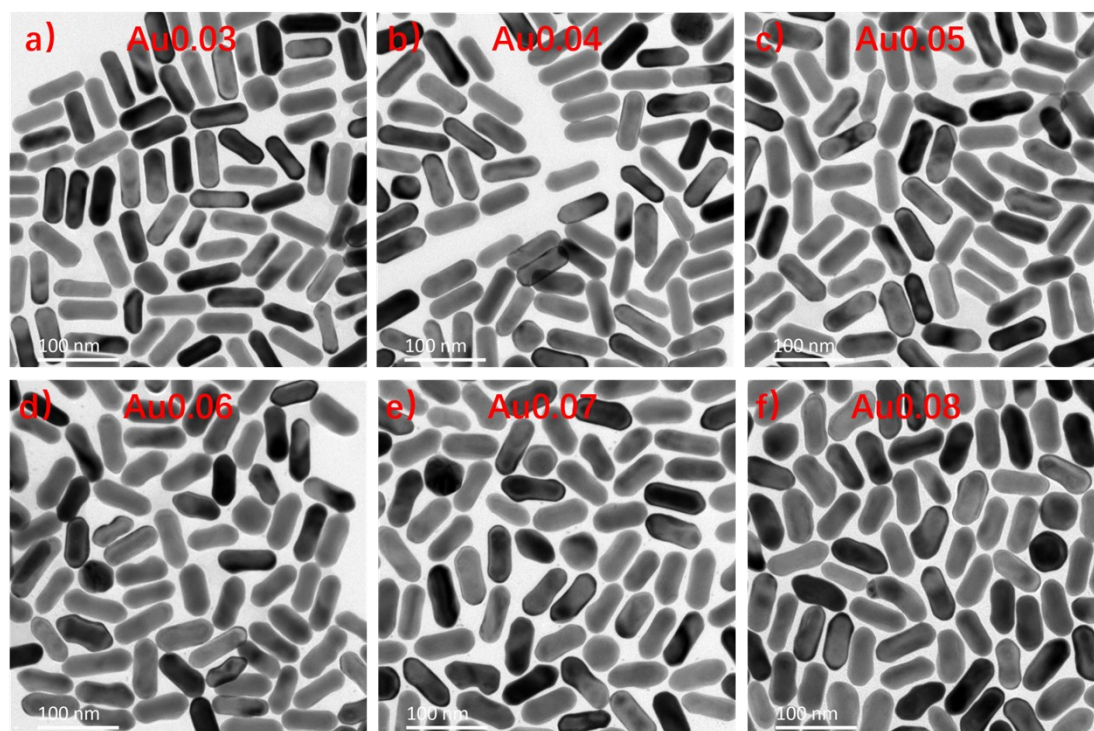
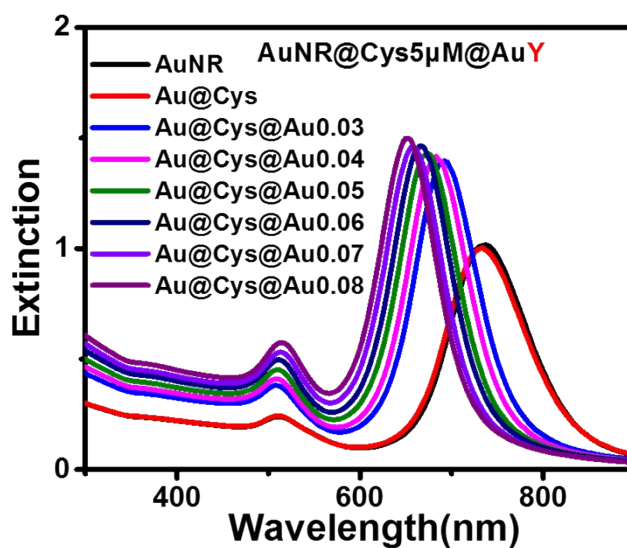
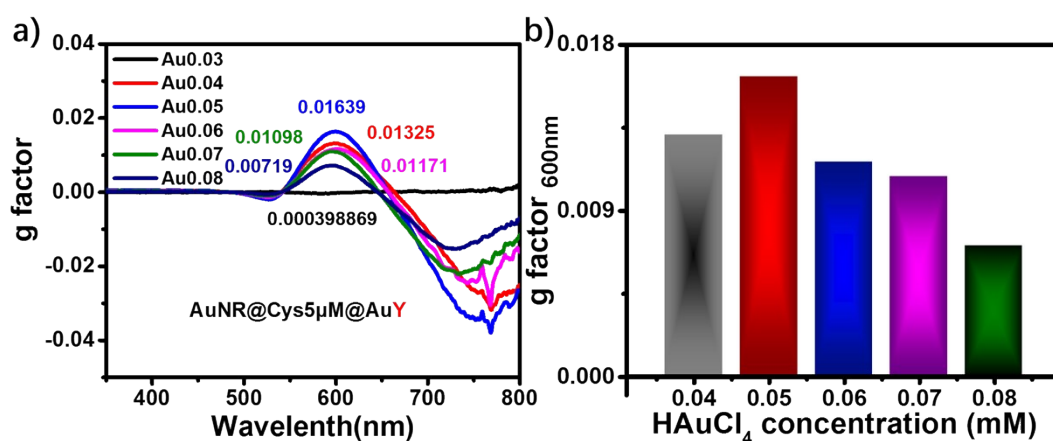


Figure S9. TEM images of AuNR@Cys5@AuY monomers.



**Figure S10.** Extinction spectra of Au@Cys5@AuY monomers with different shell thicknesses by changing HAuCl<sub>4</sub> concentration from 0.03 mM to 0.08 mM.



**Figure S11.** Effect of Au shell thickness on the PCD responses of AuNR@Cys5@AuY (Y= 0.03-0.08 mM) oligomers. (a) g factor spectra and (b) g factor value at 600 nm vs HAuCl<sub>4</sub> concentration after assembled at 60°C for 30 min.



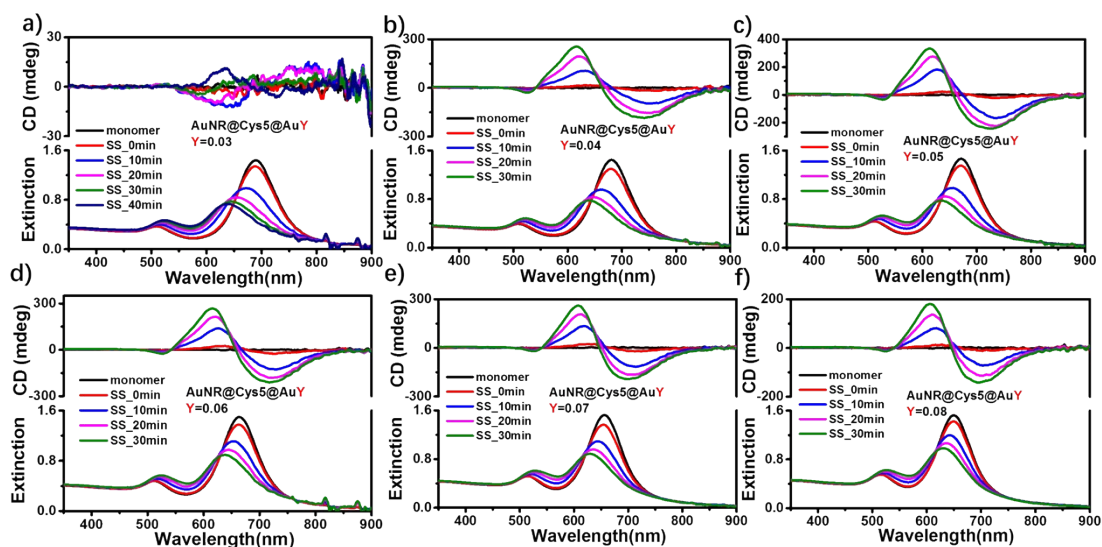


**Figure S12.** Evolutions of CD and extinction spectra of Au@Cys5@AuY ( $Y = 0.03$  to  $0.08$  mM) oligomers during  $60^\circ\text{C}$  assembly process.

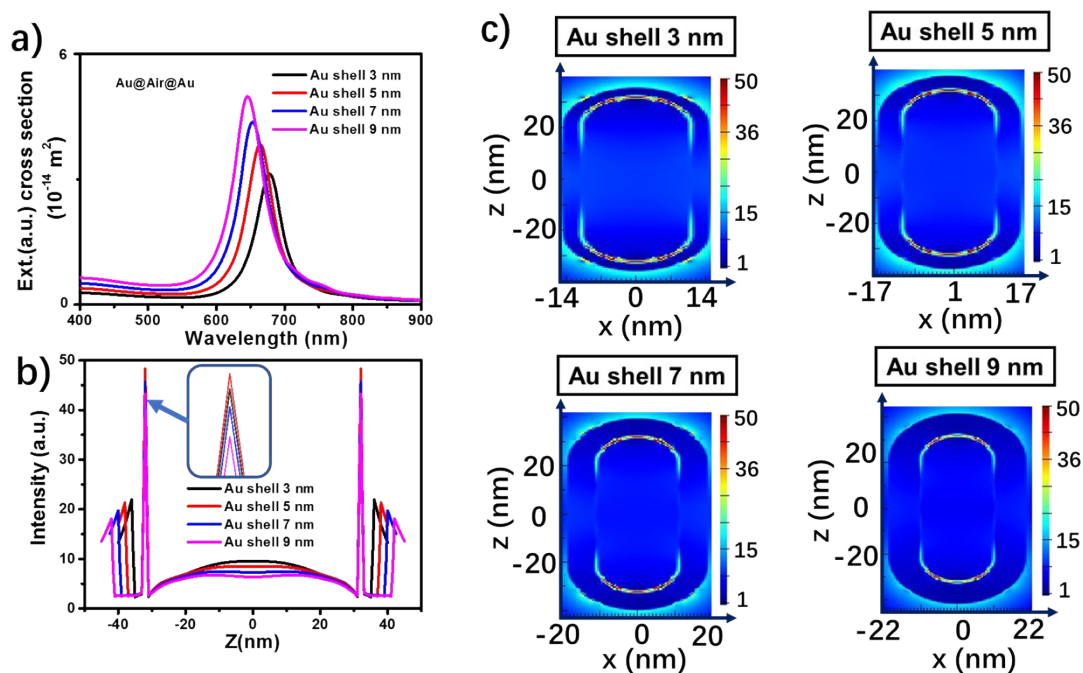


**Figure S13.** FDTD simulation of AuNR @1 nm air-gap @Au nanostructures with varying shell thickness. (a) Extinction spectra, (b) local electromagnetic field distribution along  $z$  axis, and (c) local electromagnetic field at the LSPR maximum.

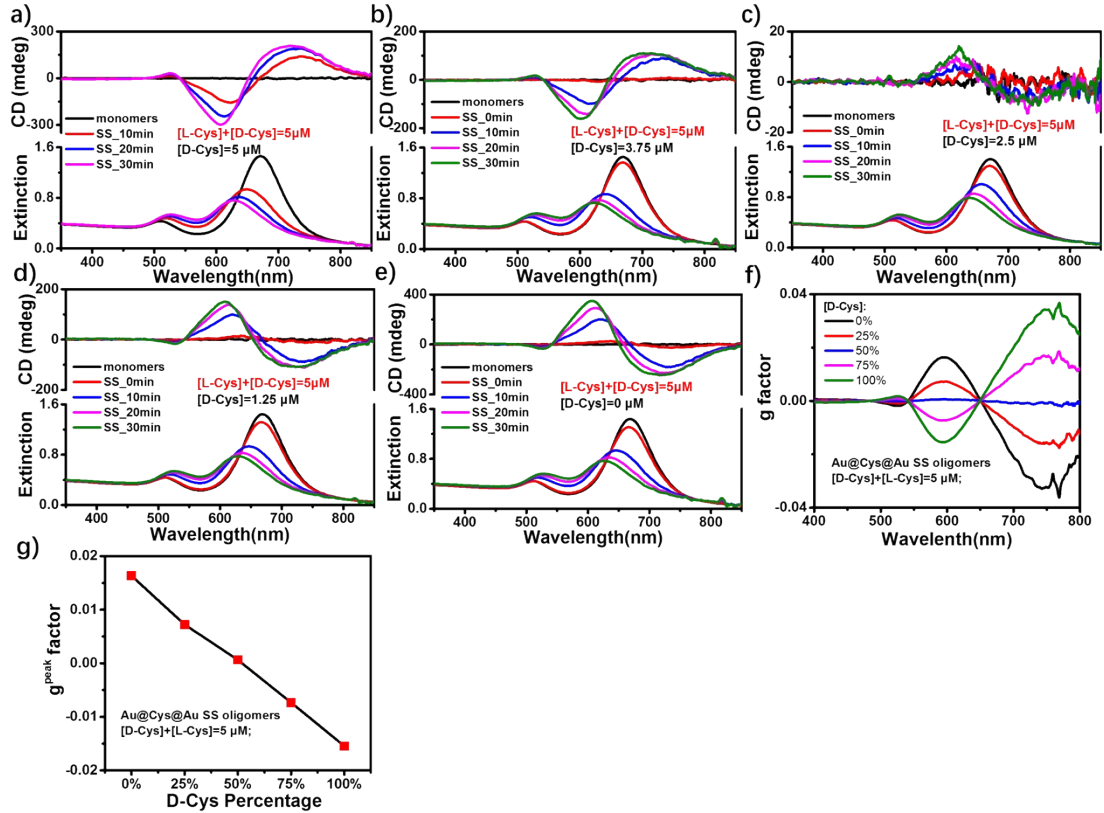


**Figure S14.** (a-e) Evolutions of CD and extinction spectra of AuNR@Cys5@Au0.05 oligomers during 60°C assembly process with L- and D-Cys molar ratio of 1, 0.75, 0.5, 0.25 and 0. (f) g factor spectra at different ee values and (g) g<sup>peak</sup> at 600 nm vs ee. [L-Cys]+[D-Cys] = 5 μM.

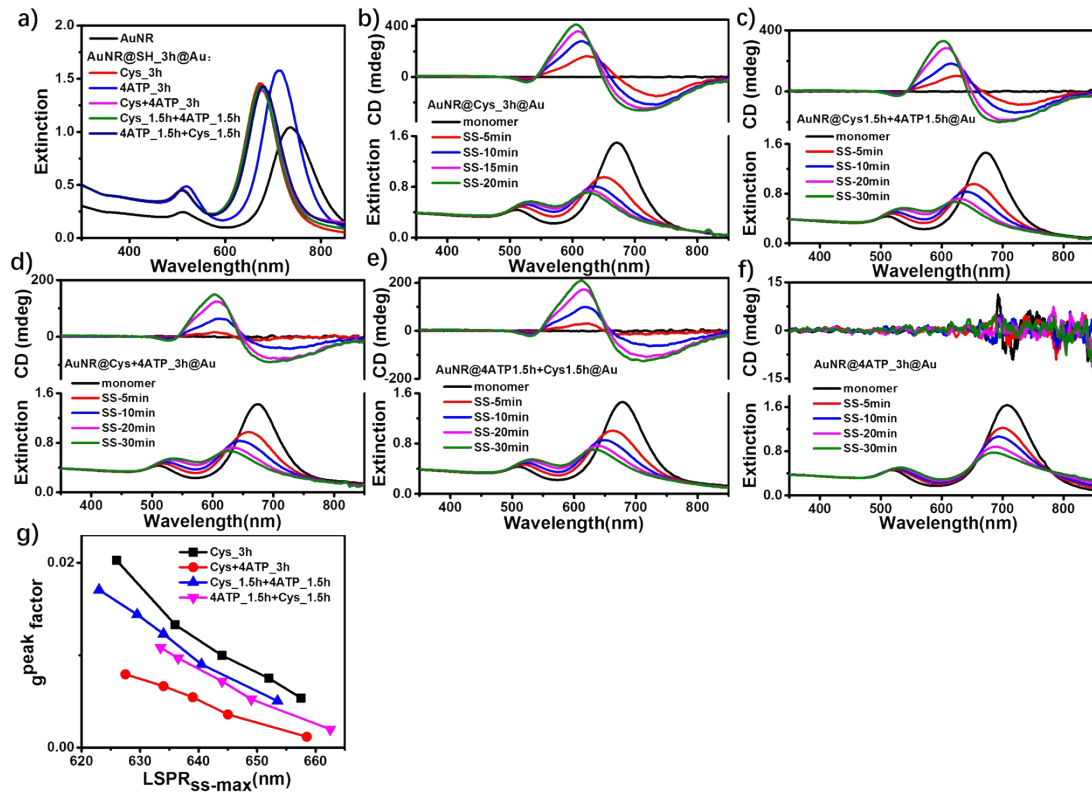


**Figure S15.** (a) Extinction spectra of AuNR@RSH@Au0.05 monomers obtained under different (4-ATP and/or Cys) incubation conditions. (b-f) Evolutions of CD and extinction spectra of AuNR@RSH@Au0.05 oligomers during 60°C assembly process. (g)  $g^{\text{peak}}$  value vs  $\text{LSPR}_{\text{SS-max}}$ . [Cys] = 2  $\mu\text{M}$ , [4-ATP] = 2  $\mu\text{M}$ .

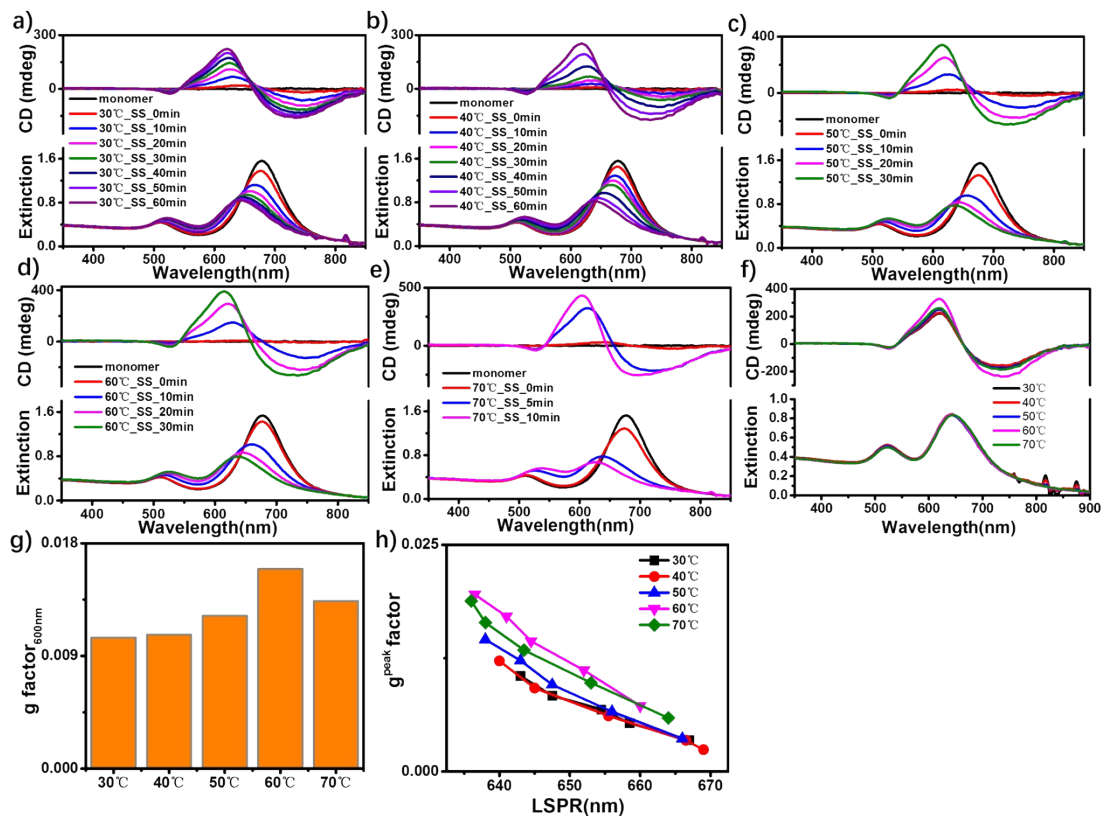


**Figure S16.** (a-e) Evolutions of CD and extinction spectra of Au@Cys5@Au0.05 oligomers during assembly process at different assembly temperatures from 30°C to 70°C. (f) The  $g^{\text{peak}}$  value vs  $\text{LSPR}_{\text{SS-max}}$  at different assembly temperatures. (g) The  $g$  factor value at 600 nm vs assembly temperature at similar assembly degrees. (h)  $g^{\text{peak}}$  value vs  $\text{LSPR}_{\text{SS-max}}$  at different assembly temperature. [CTAB] = 2 mM.

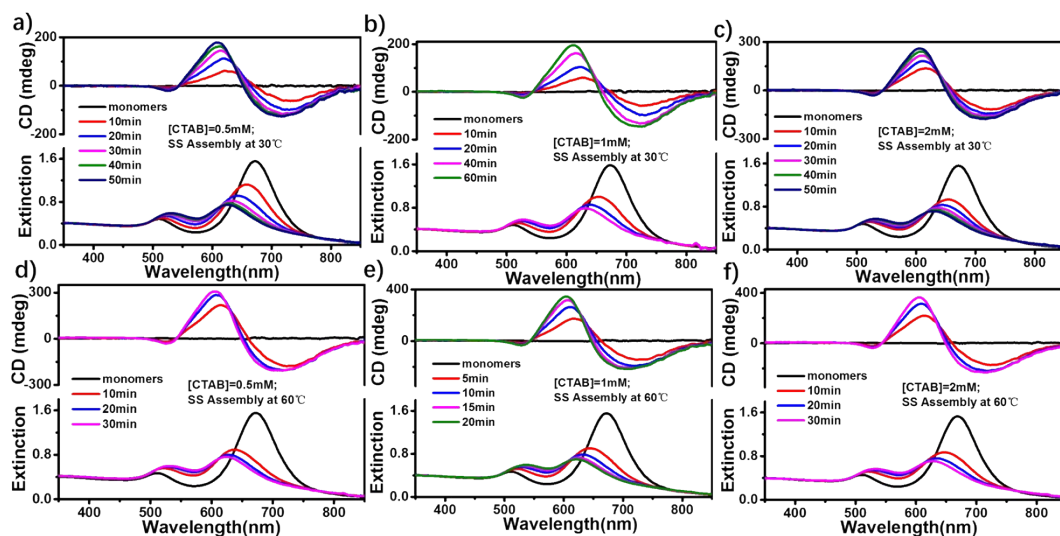




**Figure S17.** Evolutions of CD and extinction spectra of Au@Cys5@Au0.05 oligomers during SS assembly processes at 30 and 60°C, respectively, at different CTAB concentrations.

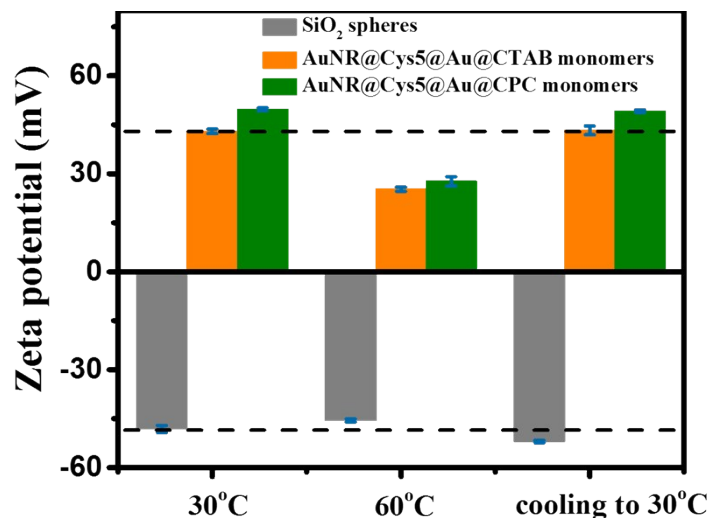


**Figure S18.** Effect of measurement temperature on Zeta potential of AuNR@Cys5@Au0.05 monomers (0.1 nM) coated with CTAB- and CPC-bilayer, respectively.

Compared with the control of negatively charged SiO<sub>2</sub> spheres, raising measuring temperature from 30°C to 60°C greatly reduced the zeta potential of AuNR@Cys5@Au0.05 monomers coated with CTAB- or CPC-bilayer. When cooling back to 30°C, the zeta potential recovered. This result indicates that enhanced Brownian motion at high temperature damages the packing order of CTAB- and CPC-bilayer on rod surface.

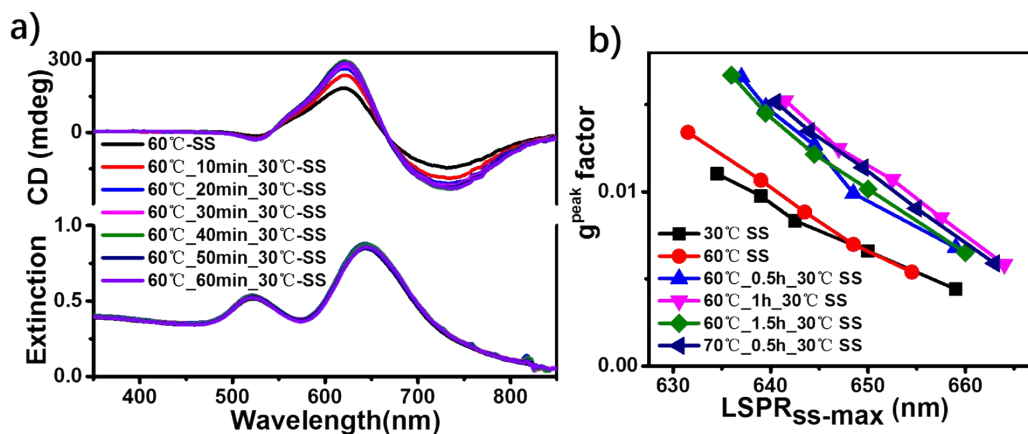


**Figure S19.** (a) CD and extinction spectra of AuNR@Cys5@Au0.05 oligomers and (b)  $g^{\text{peak}}$  value vs LSPR<sub>SS-max</sub> under different pretreatment conditions.

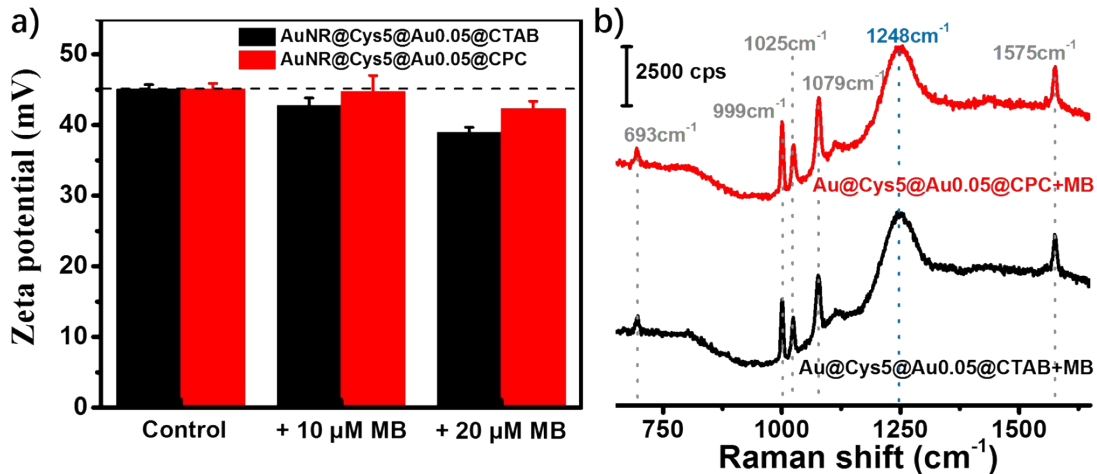


**Figure S20.** MB addition in AuNR@Cys5@Au0.05 monomers (0.1 nM) reducing Zeta potential of nanorods (a) and appearance of MB SERS signals (b) due to the adsorption of MB on rod surface. [CTAB] = 2 mM; [CPC] = 2 mM.

SERS bands at 693, 999, 1025, 1079, and 1575  $\text{cm}^{-1}$  come from adsorbed MB molecules.

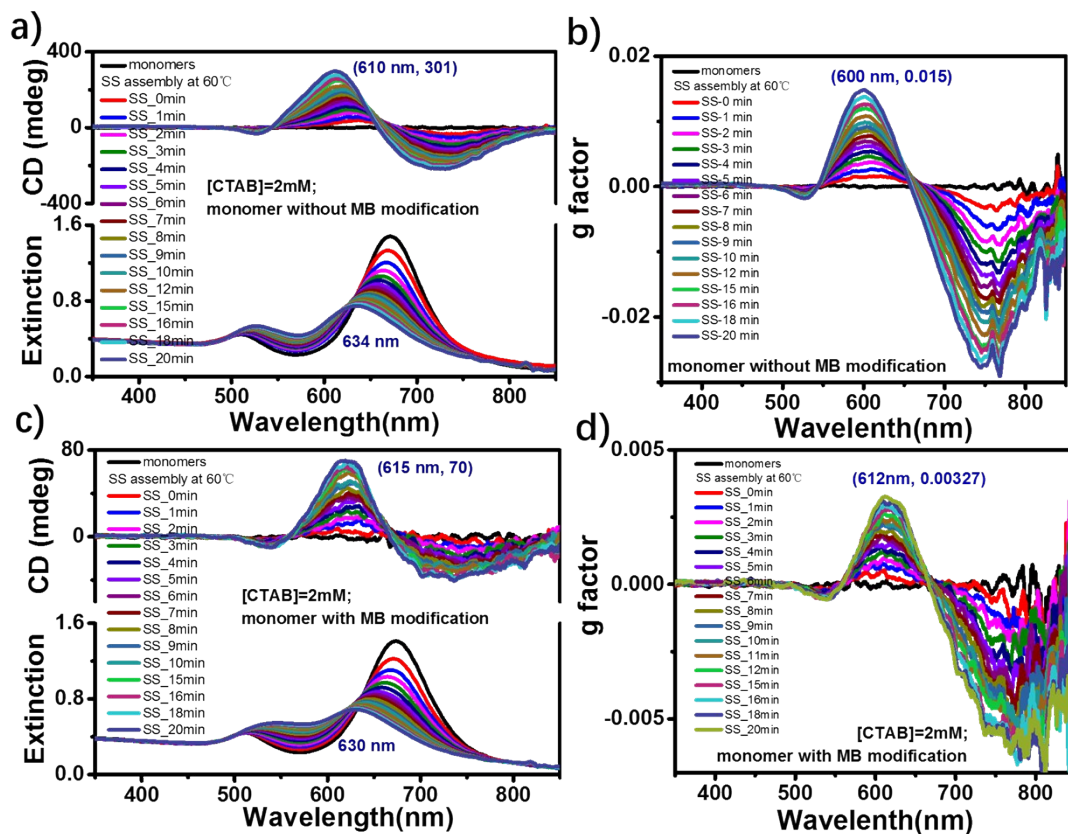


**Figure S21.** Evolutions of CD, extinction, g factor spectra of oligomers assembled at 60°C using AuNR@Cys5@Au0.05 monomers with (a and b) and without MB modification (c and d). MB modification was done by incubating 20  $\mu\text{M}$  MB with 0.1 nM AuNR@Cys5@Au0.05 monomers at 30° C for 30 min.

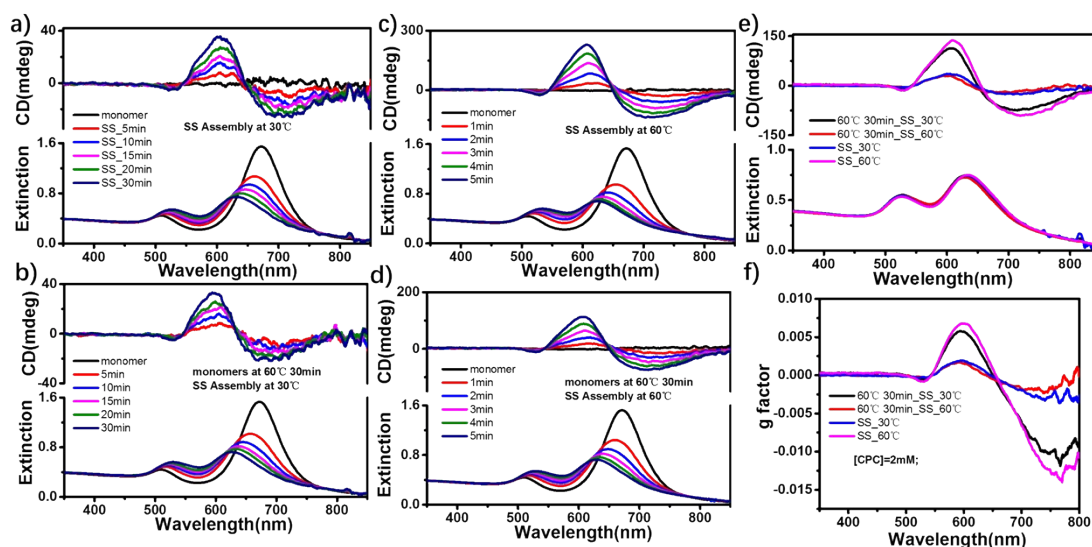


**Figure S22.** CPC as achiral surface ligands. (a-d) Evolutions of CD and extinction spectra of Au@Cys5@Au0.05 oligomers under different assembly and monomer pre-treatment conditions. e) CD and extinction spectra and (f) g factor spectra at similar assembly degrees.

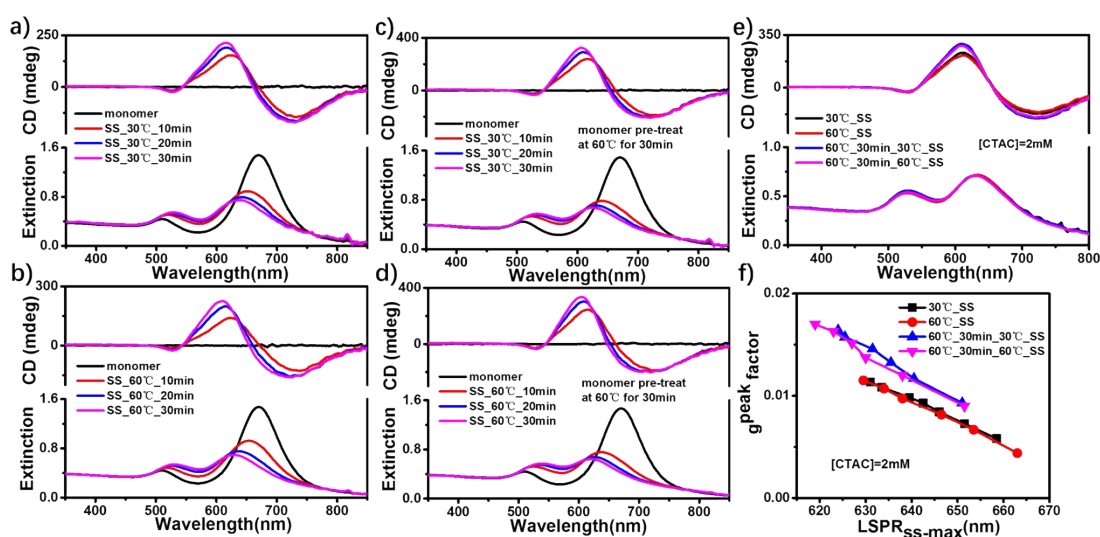


**Figure S23.** CTAC as achiral surface ligands. (a-d) Evolutions of CD and extinction spectra of Au@Cys5@Au0.05 oligomers under different assembly and monomer pre-treatment conditions. (e) CD and extinction spectra at a similar assembly degree. (f) The  $g^{\text{peak}}$  value vs LSPR<sub>SS-max</sub>.

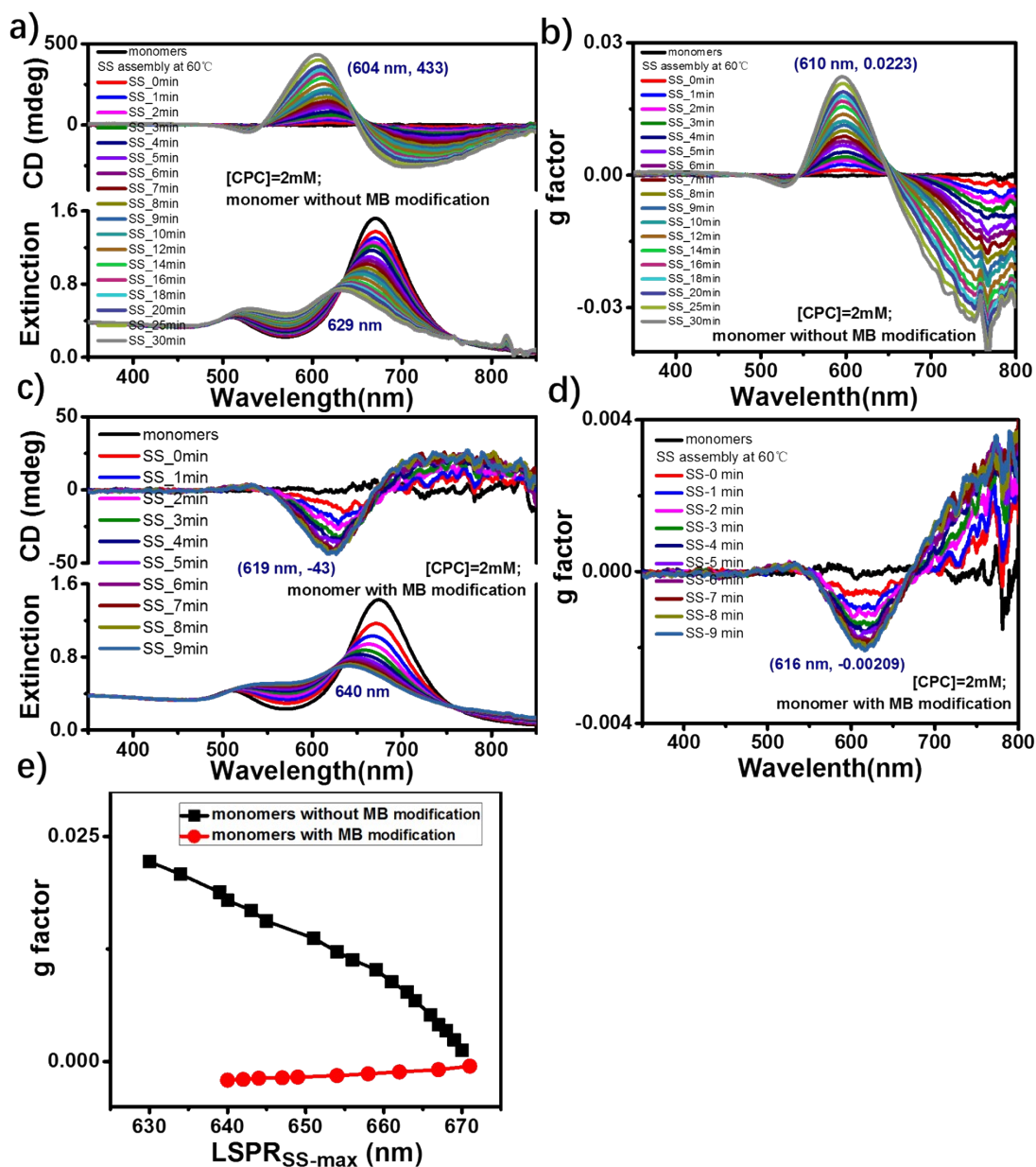


**Figure S24.** (a-d) Evolutions of CD, extinction and g factor spectra of CPC-coated AuNR@Cys5@Au0.05 SS oligomers during 60°C assembly processes with and without monomers pre-incubation with 20  $\mu\text{M}$  MB at 30°C for 30 min. (e)  $g^{\text{peak}}$  vs  $\text{LSPR}_{\text{SS-max}}$ . [CPC] = 2 mM.

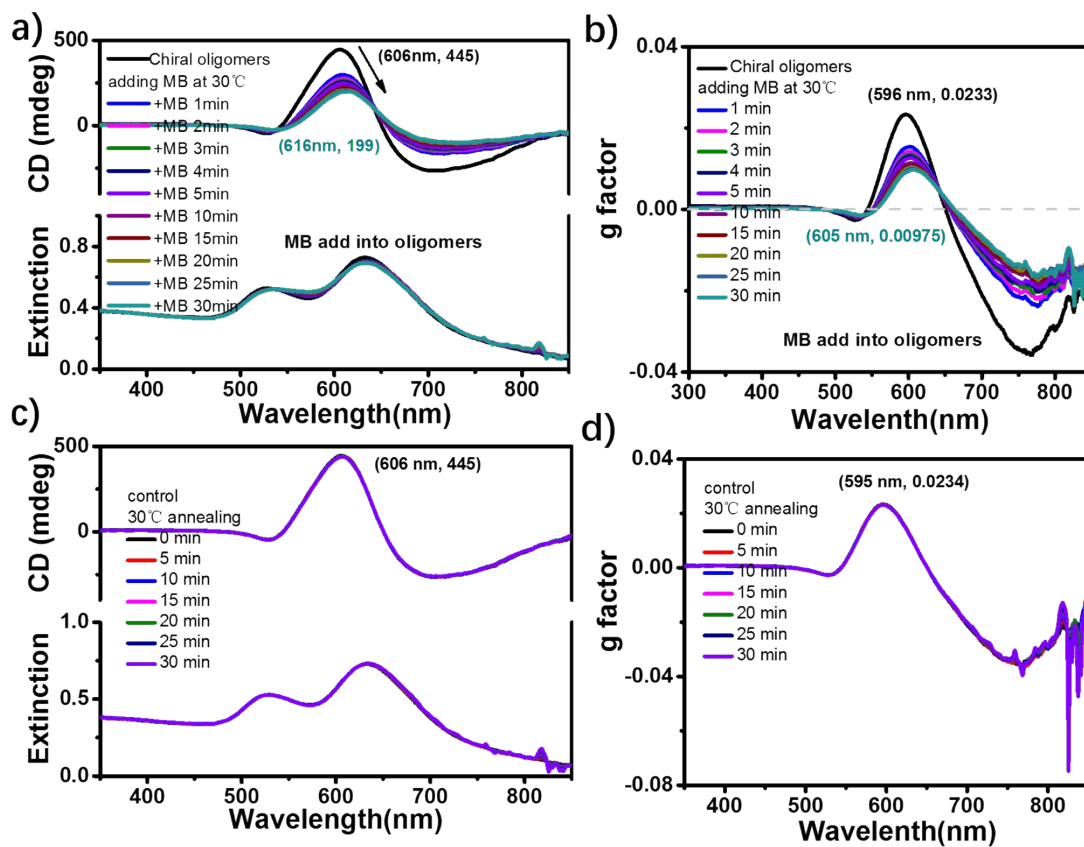


**Figure S25.** (a-d) Evolutions of CD, extinction and g factor spectra of CPC-coated AuNR@Cys5@Au0.05 chiral oligomers during 30°C annealing with and without adding 20  $\mu$ M MB. [CPC] = 2 mM.

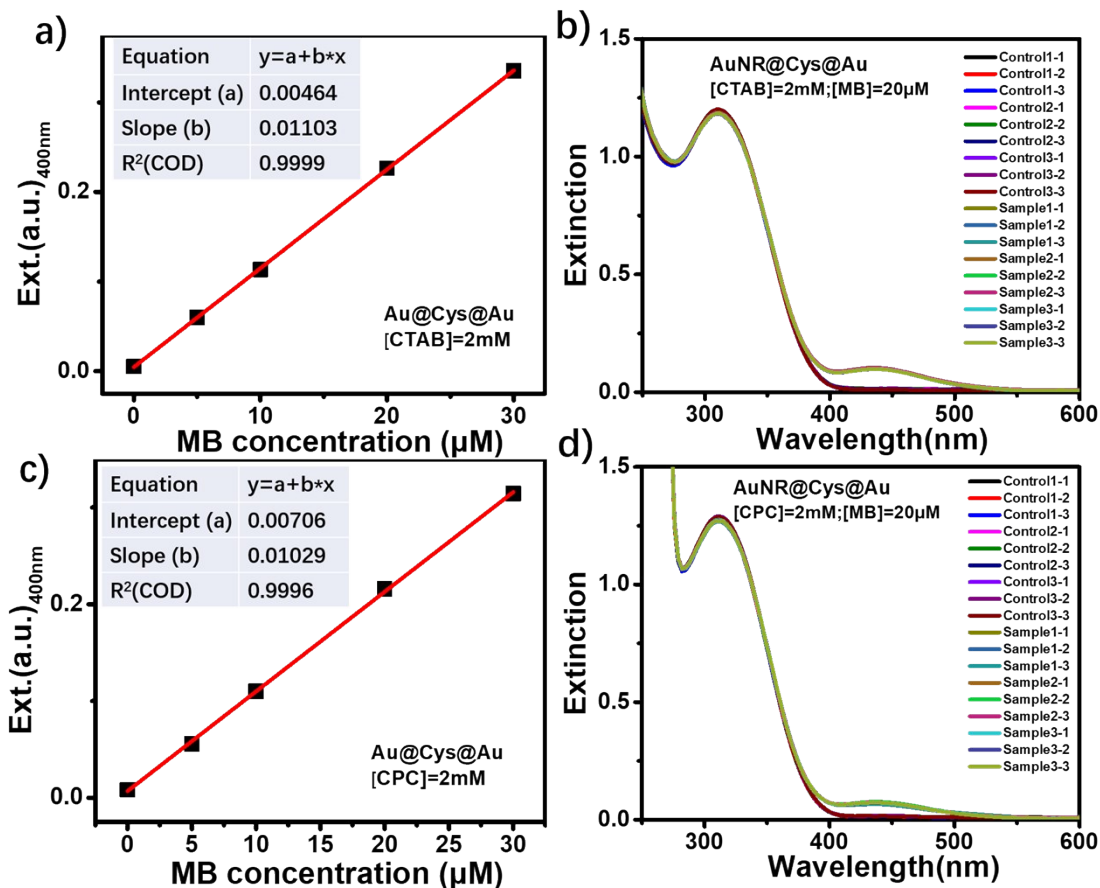


**Figure S26.** Standard curves (a and c) for determining MB adsorption amount and the extinction spectra of supernatants of CTAB- (b) or CPC-coated (d) AuNR@Cys5@Au0.05 monomers after MB adsorption. ([CTAB] or [CPC]= 2 mM, [MB]= 20 µM).

The measured MB adsorption amount of CTAB-coated and CPC-coated monomer was 10.2 µM and 13.8 µM, respectively.

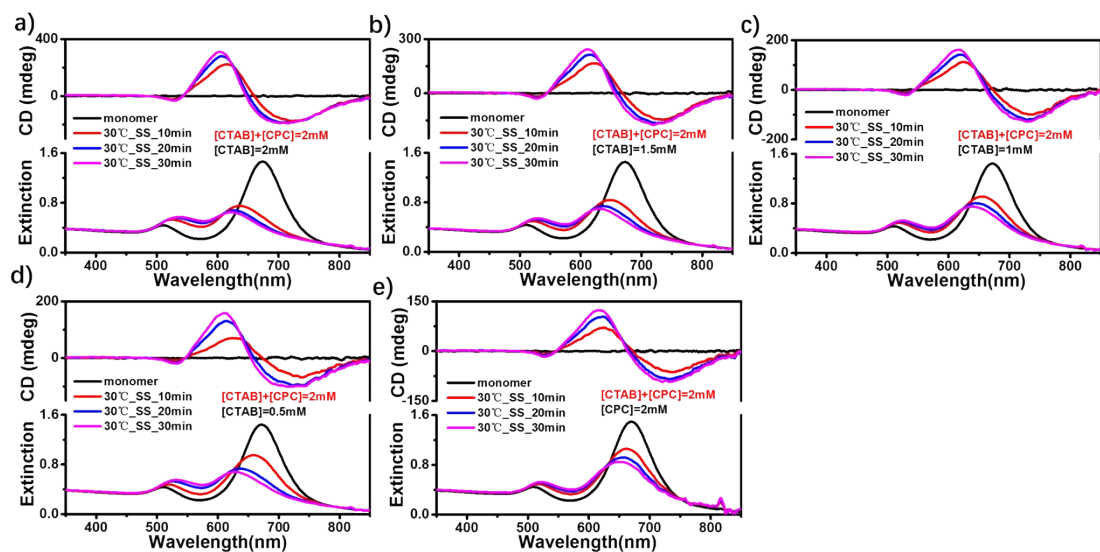


**Figure S27.** (a-e) Evolutions of CD and extinction spectra of AuNR@Cys@Au0.05 oligomers



using the mixture of CTAB and CPC as surface layer during 30°C assembly processes. [CPC] + [CTAB] = 2 mM

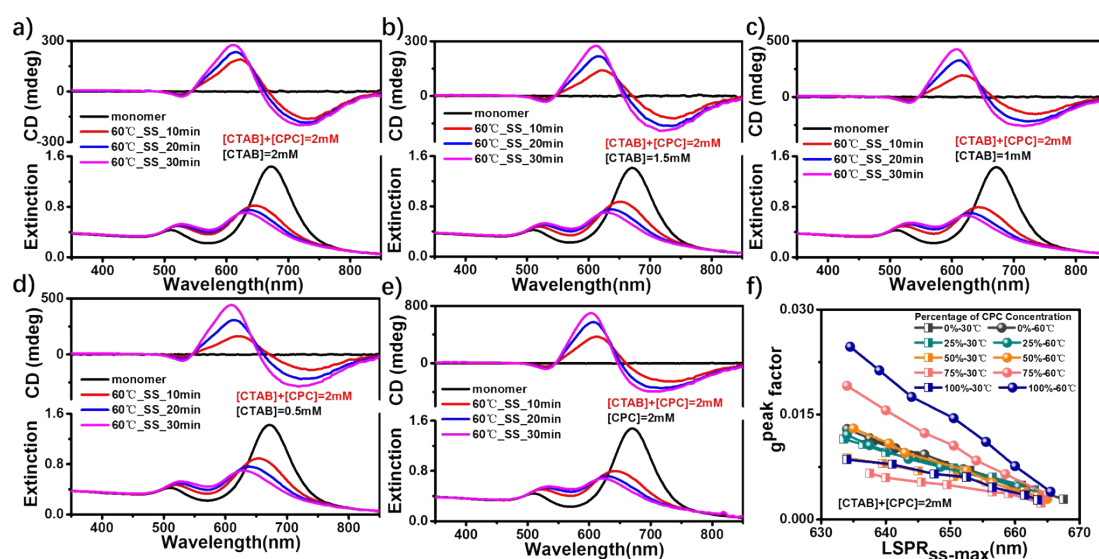


**Figure S28.** (a-e) Evolutions of CD and extinction spectra of AuNR@Cys5@Au0.05 oligomers using the mixture of CTAB and CPC as surface layer during 60°C assembly processes. [CPC] + [CTAB] = 2 mM. (f) The  $g^{\text{peak}}$  value vs LSPR<sub>SS-max</sub> at assembly temperature of 30°C and 60°C, respectively.

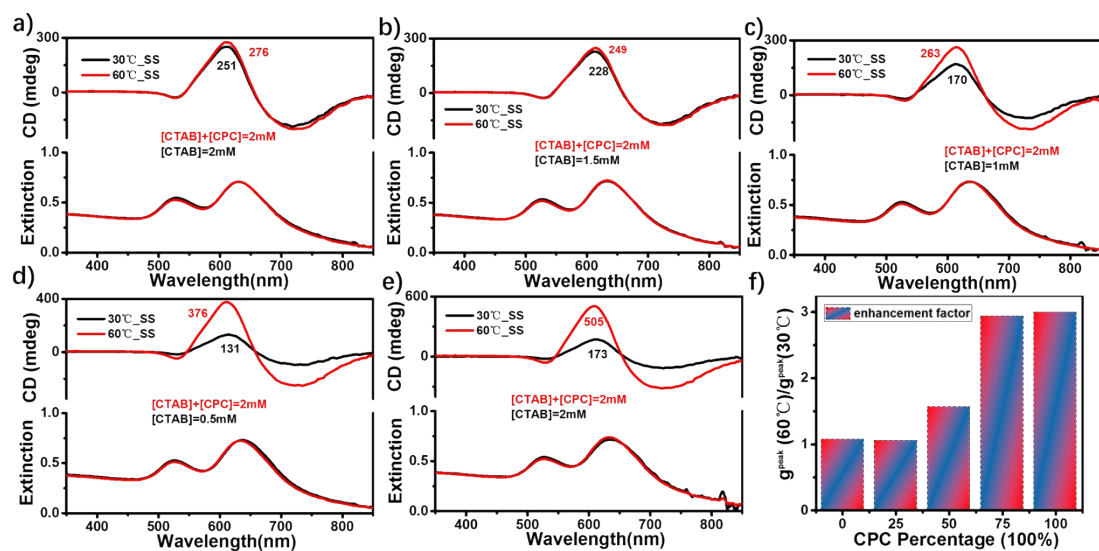


**Figure S29.** (a-e) CD and extinction spectra of AuNR@Cys5@Au0.05 oligomers using the mixture of CTAB and CPC as surface layer at similar assembly degrees. (f)  $g^{\text{peak}}(60^\circ\text{C})/g^{\text{peak}}(30^\circ\text{C})$  vs CPC percentage.

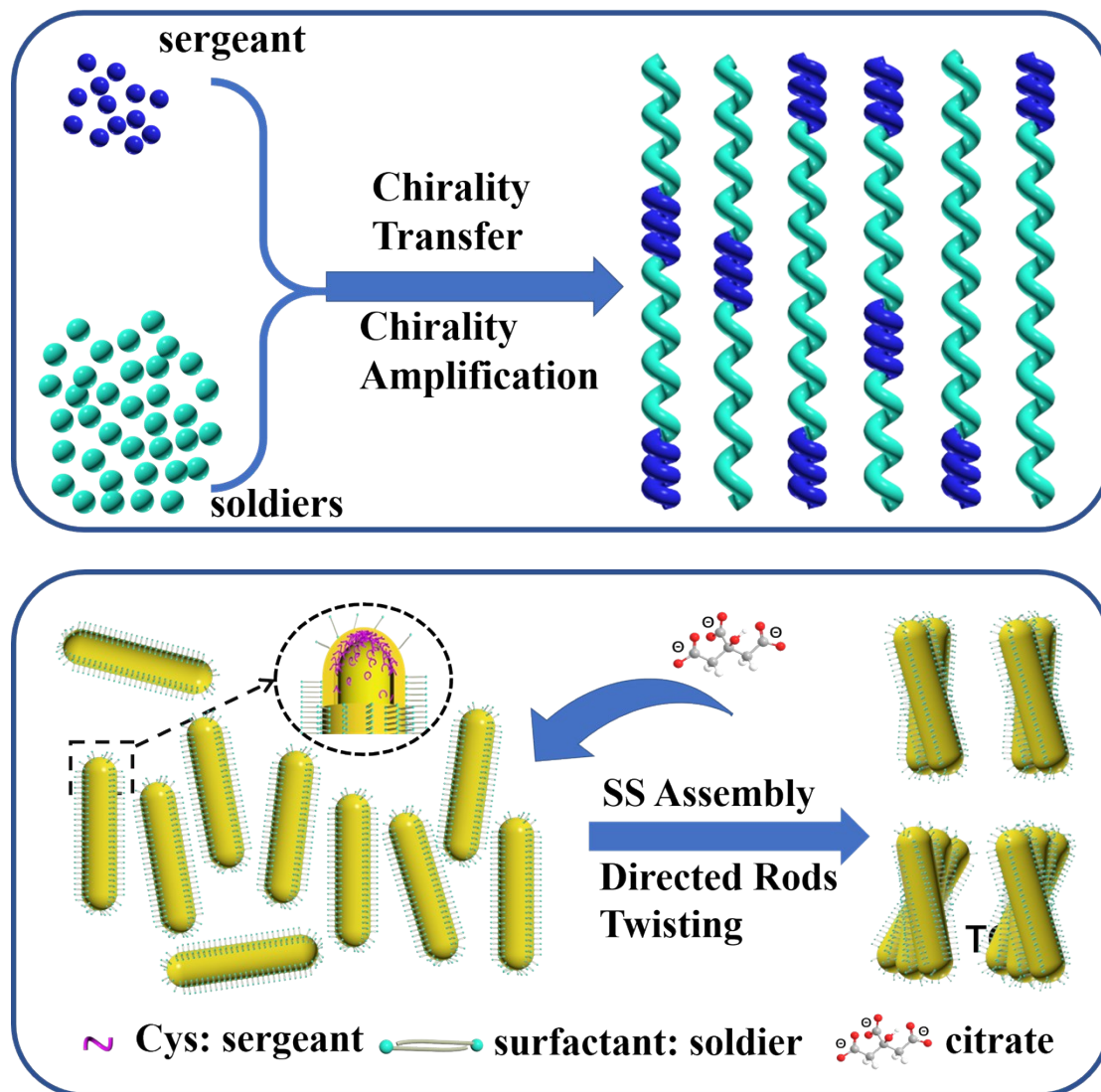


**Figure S30.** Schematic drawing of the S&S effect in supramolecular assemblies (upper panel) and in plasmonic assemblies (lower panel), respectively.